the insert corrugations to the right place in the cavity.

This adjustment has been taken into account in the following simulations shown in this paper.

5 More Realistic Start-Up Scenario

After checking the existing setup of the pre-prototype, simulations using the longer beam tunnel have been performed. Realistic multi-mode start-up simulations have been made considering the coaxial cavity with the expected magnetic field profile of the new magnet and the corresponding beam parameters using the coaxial MIG with non-emissive coating of the emitter edges at 170 GHz ($TE_{34,19}$ mode) and 204 GHz ($TE_{40,23}$ mode). The more realistic scenario considers also the non-adiabaticity of electron trajectory close to the emitter Further, the simulation results with and without non-linear uptaper have been compared to each other. Additionally, a modification of the cavity has been taken into account for an improved performance.

5.1 Simulation results at 170 GHz using the existing coaxial-cavity design

Firstly, ARIADNE simulations using the new magnetic field profile have been performed and the obtained electron beam parameters have been used in EURIDICE. In this simulation, at 170 GHz the alpha spread is $\Delta\alpha = 6.08$ % for $\alpha = 1.3$. The energy spread amounts to 0.08 % and the kinetic energy spread to 0.12 %. The realistic start-up scenario at 6.86 T without non-linear uptaper is shown in Fig. 4. Taking the wall loading constraint into account, the operation parameters are $U_{beam} = 89$ keV and $I_{beam} = 75$ A, where the tube can deliver an RF output power of 2.3 MW at an interaction efficiency of 36.7 %. Initial studies including the non-linear uptaper after the cavity have been started. Figure 5 presents the start-up scenario using the same parameters as mentioned before for a better comparison. The shown start-up is not that smooth as before, but nevertheless the nominal $TE_{34,19}$ mode is finally excited. The wall loading constraint limits the operation to $U_{beam} = 90$ keV. The RF output power decreases to 2.25 MW at an interaction efficiency of 34 % and an insert loading of 0.12 kW/cm^2.

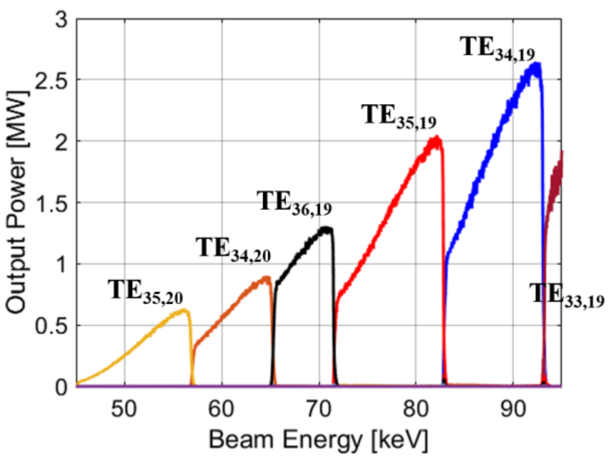

Fig. 3. Realistic start-up scenario with existing coaxial cavity at 6.86 T and $I_{beam} = 75$ A without non-linear uptaper using the magnetic field profile proposal from the new SC magnet and the gun parameters from the new coaxial MIG.

5.2 Simulation results at 204 GHz using the existing coaxial-cavity design

The coaxial MIG with non-emissive coating of the emitter edge have been simulated via ARIADNE for the operation at 204 GHz using the new magnet. The gun parameters have been selected to give a pitch factor of $\alpha = 1.2$ having an alpha spread of $\Delta\alpha = 4.3$ % and a kinetic energy spread of 0.1 %. The simulation shows a good scenario starting with the $TE_{-40,24}$ mode at ~48 keV in Fig. 6, where the minus refers to a counter-rotating mode. Starting from 60 keV the $TE_{41,23}$ mode is excited while the nominal $TE_{40,23}$ mode is getting dominant at ~75 keV. Starting from 83 keV the competing $TE_{-38,23}$ mode, which has nearly the same caustic radius, is getting stronger and so the nominal mode collapses. The operation is limited to 79.2 keV due to the wall loading constraint. The cavity delivers 1.7 MW RF output power without non-linear uptaper at an interaction efficiency of

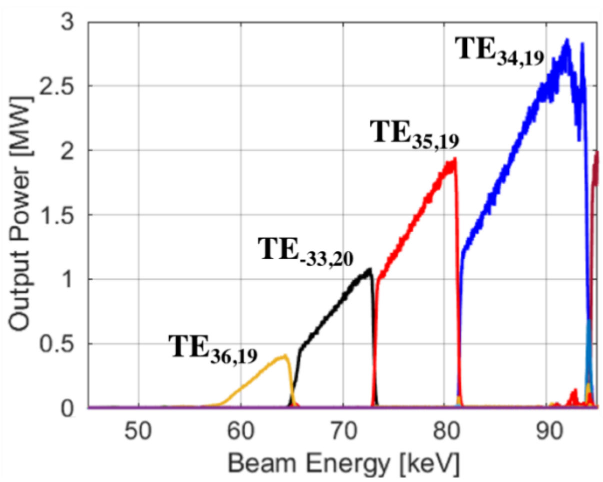

Fig. 4. Realistic start-up scenario with the existing coaxial cavity at 6.86 T and $I_{beam} = 75$ A without non-linear uptaper using the magnetic field profile proposal from the new SC magnet and the gun parameters from the new coaxial MIG.

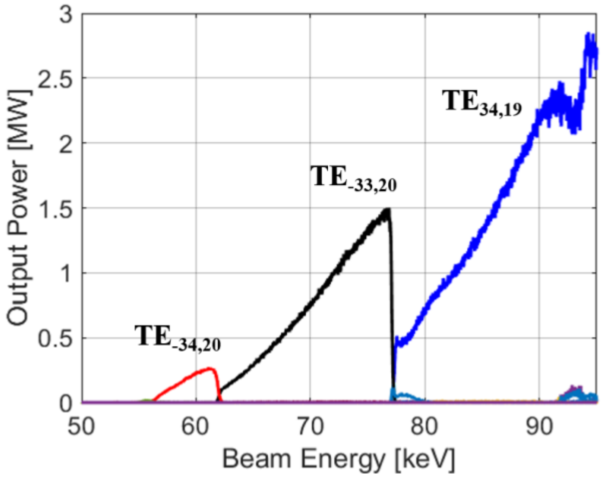

Fig. 5. Realistic start-up scenario with existing coaxial cavity at 6.86 T and $I_{beam} = 75$ A with non-linear uptaper using the magnetic field profile proposal from the new SC magnet and the gun parameters from the new coaxial MIG.

33 % and an insert loading of 0.06 kW/cm². The delivered RF output power is 0.1 MW lower than the results presented in section 3.

Initial studies considering also the influence of the non-linear uptaper at 204 GHz are being performed. Figure 7 presents the start-up scenario using the same parameters as mentioned before for comparing the results to each other. The scenario looks quite similar with and without the non-linear uptaper, as it should. The point at which the $TE_{40,23}$-mode collapses is nearly identical as before. Additionally, the $TE_{41,22}$ mode oscillates after the $TE_{40,22}$ mode. The delivered RF output power and the interaction efficiency are not influenced by the non-linear uptaper.

5.3 Further modifications

In order to get a dual-frequency gyrotron delivering 2 MW, or even more at both operation frequencies, modifications have to be done. For this reason, the cavity midsection length has been reduced from 16 mm to 13.6 mm, as mentioned in the previous section. The start-up simulation of the shortened cavity for the $TE_{34,19}$-mode case is shown in Fig. 8. Concerning the nominal operation parameters of U_{beam} = 90 keV and I_{beam} = 75 A and an increased magnetic field of 6.88 T, the cavity delivers 2.4 MW RF output power at an interaction efficiency of 37 % having a wall loading of 1.9 kW/cm². Compared with the longer cavity, the gyrotron can deliver 0.1 MW more RF output power with an increased interaction efficiency of ~1 percentage point at this operating point. However, concerning the Ohmic wall loading constraint the nominal operation point could be extended to U_{beam} = 90.6 keV, where the cavity delivers 2.5 MW at an efficiency of 38.2 %.

This modification has to be proven for the 204 GHz operation, as well. The simulation shows a good scenario starting with the $TE_{42,23}$ mode, over the $TE_{41,23}$ mode and finally the nominal $TE_{40,23}$ mode is excited until the competing $TE_{-38,23}$ mode raises, as shown in Fig. 9. The operation point is found by the wall loading constraint and is determined by U_{beam} = 86.5 keV, having an RF output power of 2.06 MW at an interaction efficiency of 33.5 %. Comparing these results with the existing cavity design, the RF output power can be increased by ~0.4 MW and the interaction efficiency by 0.5 percentage points.

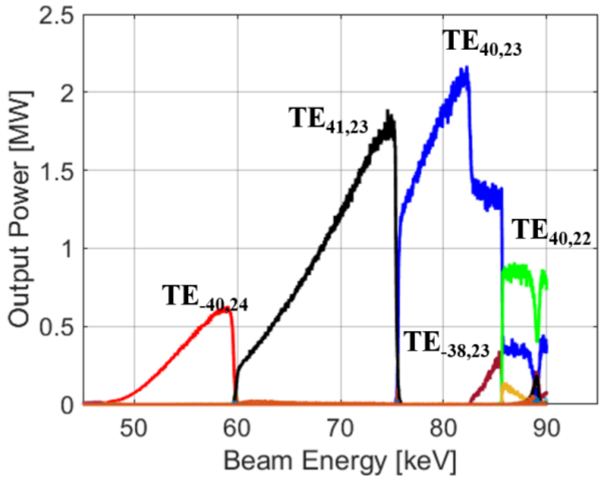

Fig. 6. Realistic start-up scenario with the existing coaxial cavity at 8.15 T and I_{beam} = 70 A without non-linear uptaper using the magnetic field profile proposal from the new SC magnet and the gun parameters from the new coaxial MIG.

6 Multi-Frequency Launcher Design

The operating modes excited in the cavity are converted into the fundamental Gaussian mode using an internal quasi-optical mode converter which contains a mirror-line launcher and three mirrors. The existing single frequency (170 GHz) launcher design is already presented in [10]. The simulation results show that in the case of fabrication error on the wall perturbation of ± 10 µm, the launcher will still provide a RF beam with high Gaussian mode content. The measurement results are in a quit good agreement with the simulations. The simulated fundamental Gaussian mode content is determined by 96.3 % at the launcher aperture at 170 GHz [17].

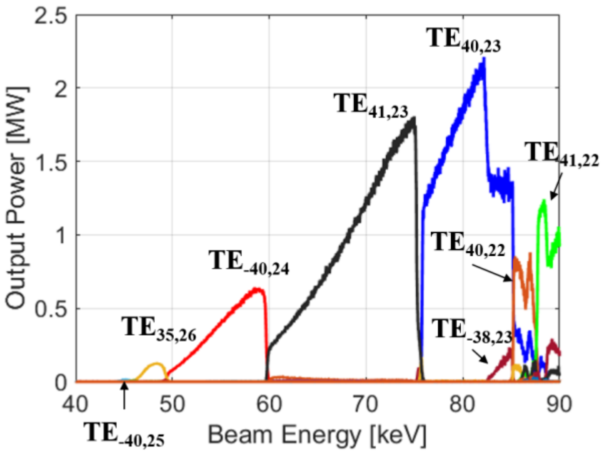

Fig. 7. Realistic start-up scenario with the existing coaxial cavity at 8.15 T and I_{beam} = 70 A including the non-linear uptaper using the magnetic field profile proposal from the new SC magnet and the gun parameters from the new coaxial MIG.

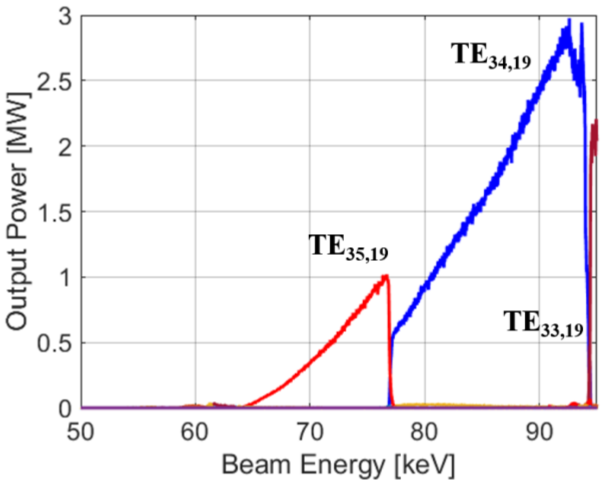

Fig. 8. Realistic start-up scenario with a shortened coaxial cavity length at 6.88 T and I_{beam} = 75 A using the magnetic field profile proposal from the new SC magnet and the gun parameters from the new coaxial MIG.

Table 2. Summary of the realistic multi-mode simulation results using EURIDICE using the new Tesla magnet configuration.

Mode	$TE_{34,19}$			$TE_{40,23}$		
Configuration	w.o. uptaper	w. uptaper	modification	w.o. uptaper	w. uptaper	modification
Frequency [GHz]	170.005	170.020	170.041	204.145	204.141	204.167
Beam voltage [keV]	90	90	90.6	79.2	79.2	86.5
Beam current [A]	75	75	75	70	70	75
Magnetic field [T]	6.86	6.86	6.88	8.15	8.15	8.23
Velocity ratio, α	1.3	1.3	1.3	1.2	1.2	1.2
Interaction length [mm]	16.0	16.0	13.6	16.0	16.0	13.6
Wall loading [kW/cm^2]	1.89	2.00	2.00	2.00	2.00	2.00
Insert loading [kW/cm^2]	0.11	0.11	0.13	0.06	0.06	0.07
RF output power [MW]	2.3	2.2	2.5	1.7	1.7	2.06
Interaction eff. [%]	36.7	34.0	38.2	33	33	33.5

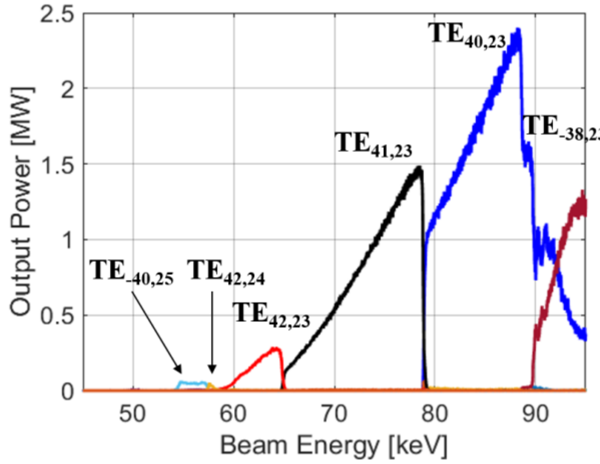

Fig. 9. Realistic start-up scenario with a shortened coaxial cavity midsection length at 8.23 T and I_{beam} = 75 A.

Having a dual frequency scenario, the existing mirror-line launcher with radius of 32.5 mm is tested to assess whether the performance is good enough at 204 GHz. First initial studies at 204 GHz for the $TE_{40,23}$ mode show a fundamental Gaussian mode content of only 91.6 % at the launcher aperture. Therefore, a new launcher was designed with good performance operating both at 170 GHz and 204 GHz. The new launcher is also a mirror-line launcher, and its radius is 32 mm. This dual-frequency launcher design shows promising results despite the difference of the modes' caustic radii of around 2 %. The Gaussian mode content was calculated to be 97.2 % at 170 GHz and 96.6 % at 204 GHz.

7 Summary and Outlook

The simulations of this paper show that the existing KIT $TE_{34,19}$-mode coaxial-cavity pre-prototype gyrotron could operate in the KIT FULGOR gyrotron test stand using the new 10.5 T magnet, under the assumption of enlarge the beam tunnel. Furthermore, the adapted gyrotron is capable of operation as a multi-purpose/multi-frequency device. Without any other modifications the simulations show that the gyrotron delivers at 204 GHz (170 GHz) 1.7 MW (2.3 MW) at an interaction efficiency of 33 % (36.7 %). A small modification of the cavity length would increase the RF output power by 0.4 MW and the interaction efficiency by 0.5 percentage points at 204 GHz. Operating a dual-frequency coaxial-cavity gyrotron in the new test stand, the following aspects have to be taken into account: (i) the gyrotron length has to be adjusted due to the height of the new magnet, (ii) as a consequence to this, the coaxial insert has to be modified by the same length, (iii) in principle the cavity can operate at both frequencies, but with a small reduction of the cavity length the results can be improved, and (iv) the launcher has to be improved for sufficient performance at 204 GHz.

This work has been carried out within the framework of the EUROfusion Consortium and has received funding from the Euratom research and training programme 2014-2018 under grant agreement No. 633053. The views and opinions expressed herein do not necessarily reflect those of the European Commission. Part of the simulations were performed on the EUROfusion High Performance Computer (Marconi-Fusion).

References

1. H. Braune, et al., *In Proc. IRMMW* (2016).
2. T. Omori, *et al.*, *Fusion Eng. Des.*, (2011).
3. G. Federici, *et al.*, in *Proc. 25th SOFE*, (2013).
4. Z. C. Ioannidis *et al.*, *IEEE Trans. on Electron Devices*, (2017).
5. P. C. Kalaria, *et al.*, *Physics of Plasma*, 23(9), 2016.
6. C. T. Iatrou, *et al.*, *IEEE Trans. Microwave Theory Tech.*, (1996).
7. K. A. Avramides, *et al.*, "*IEEE Trans. on Plasma Science*, (2004).
8. T. Rzesnicki, et al., "*IEEE Trans. on Plasma Science,* (2010).
9. S. Illy, *et al.,* EC-20 workshop, (2018).
10. S. Ruess, *et al.* , 47th EUMC, (2017).
11. M. Schmid et al., Fus. Eng. Des. **123**, 485, 2017.
12. T. Ruess, *et al.*, GeMiC (2018).
13. K. A. Avramides, *et al.*, EC-17 *Workshop (*2012).
14. K. A. Avramidis *et al.*, *IRMMW-THz*, Copenhagen, 2016, pp. 1-2.
15. I. Gr. Pagonakis, S. Illy, M. Thumm, *Physics of Plasmas*, 23, 83103 (2016).
16. I. Gr. Pagonakis and J. L. Vomvoridis. *IRMMW (*2004).
17. J. Jin, *et al.*, in *IEEE Trans. on Microwave Theory and Techniques* (2009).